ISSN 2176-5480

22nd International Congress of Mechanical Engineering (COBEM 2013)
November 3-7, 2013, Ribeirão Preto, SP, Brazil

NUMERICAL STUDY OF THE HEAT TRANSFER PROCESS IN A SOLAR FRUIT DRYER WORKING IN NATURAL CONVECTION

Luiz Guilherme Vieira Meira Souza
UFRN - Universidade Federal do Rio Grande do Norte, Campus Universitário Lagoa Nova, CEP 59078-970, Natal/RN – Brasil
lguilherme_souza@hotmail.com

Sandi Itamar Schafer de Souza
UFRN - Universidade Federal do Rio Grande do Norte, Campus Universitário Lagoa Nova, CEP 59078-970, Natal/RN – Brasil
sandi@ufrnet.br

Luiz Guilherme Meira Souza
UFRN - Universidade Federal do Rio Grande do Norte, Campus Universitário Lagoa Nova, CEP 59078-970, Natal/RN – Brasil
lguilherme@dem.ufrn.br

Maria Kalionara de Freitas Mota
UFRN - Universidade Federal do Rio Grande do Norte, Campus Universitário Lagoa Nova, CEP 59078-970, Natal/RN – Brasil
kalionarafreitas@yahoo.com.br

Amanda Gonçalves Cavalcante
UFRN - Universidade Federal do Rio Grande do Norte, Campus Universitário Lagoa Nova, CEP 59078-970, Natal/RN – Brasil
amandacavalcante_123@hotmail.com

Abstract. *It's presented a numerical study of a solar fruit dryer, which works in natural convection, using a CFD (Computational Fluid Dynamics) simulation in a model developed in commercial packs. Obtained data from computational simulations like thermal and pressure gradients will be useful to evaluate Nusselt and Rayleigh numbers behaviors, involved in such heat transfer process, and use them to optimize the thermal performance of the model, ensuring that building a real model of this dryer based on these results is feasible. Also, it's necessary a study on a more applicable turbulence model aiming to choose an adequate one to be used considering the flow characteristics involved in this analysis.*

Keywords: *solar fruit dryer, computational simulations, heat transfer*

1. INTRODUCTION

For thousands of years people have sundried fruit and vegetables to preserve for leaner times. New technologies brought changed techniques but, at present, the increasing demand for healthy and low-cost natural foods and the need for sustainable income are bringing solar drying to the fore as a useful alternative for surplus products.

The great challenge of the globalized world is currently producing food for a population that continues to grow and reaches six and a half billion inhabitants. Since farmlands are shrinking, the supply of irrigation water is scarce and production technologies are no longer able to give more leaps in productivity, it is believed that in the next decades the food supply in the world will grow unless the population.

Brazil is an exception in this panorama and stands as one of the forces producing the third millennium. Currently, Brazil is the third largest fruit producer in the world, behind China (157 million tons) and India (54 million). Of the 39 million tons of fruit produced, approximately 45% is orange. Secondly, there is the banana, with 6.5 million tons (Anuário Brasileiro de Frutas, 2005).

The Brazilian fruit market moves now over 10 billion dollars a year (only with fresh fruit) and generates products of medium and high added-value, considering the fruit exploitation for exportation and noble fruit. Brazil's climate permits the production of all kinds of tropical fruit and some provide more than a crop per year.

Given the importance of drying fruit not only as a growing industry, with a promising future in countries like Brazil, but also as a way to overcome this lack of productivity leaps, it is necessary to optimize the processes and reduce the costs, causing an increase in the dynamic market of dried fruit.

This work aims at a numerical study of a fruit solar dryer working on natural convection built in composite material developed at UFRN on LMHES (Laboratorio de Maquinas Hidraulicas e Energia Solar). The objective is to create, study and, if possible, optimize a computational model of this equipment. It will be performed an analysis of its current working and efficiency, based on pressure gradients, analysis of specified temperatures, velocity vectors, and mass flows within it. This will be performed using CFD (Computational Fluid Dynamics), seeking that by the end of work an improved model that can be used for development of future equipment can be obtained.

ISSN 2176-5480

The study also includes a study of turbulence transition in thermal boundary layers and the system working regime, in addition to experimental measurements performed in the already built dryer, so the model can be fed with as near as possible to the real data.

2. BIBLIOGRAPHIC REVISION

Dehydration is a process which combines heat and mass transfer, reducing the quantity of water in food, increasing its durability and avoiding their waste. The advantages of drying food include: dried products improve family nutrition because fruit and vegetables contain high quantities of vitamins, minerals and fibers; for diabetics dried fruit prepared without adding sugar is a healthy choice instead of desserts; dried fruit can be used in stews and soups or enjoyed as snacks. It can also be added to cereals for breakfast or used in making ice cream and baked products; it improves the value of the product; the product carriage is facilitated. (Meloni, 2002).

The solar drying is one of the most promising uses and most far-reaching social primary source that makes life possible on Earth. In Brazil for several decades researchers have been studying many types of dryers to promote the dehydration of numerous types of food. Names such as Camera Cleanto Torres, Arnaldo Moura Bezerra, Fioreze Romeo, Antonio Raimundo Costa, G. Roa and others have made the solar drying a reality in our country.

According to Meloni (2005), it is necessary to supply heat to evaporate the humidity of the product and a mean of transport to remove the water vapor formed on the surface of the product to be dried. The airflow in the drying chamber, serves to carry the moisture removed from the product to the environment. The removal of moisture in the product can be obtained by natural convection (such as the studied dryer) or by forced convection using a fan or blower. Figure 1 illustrates the case of drying by natural convection.

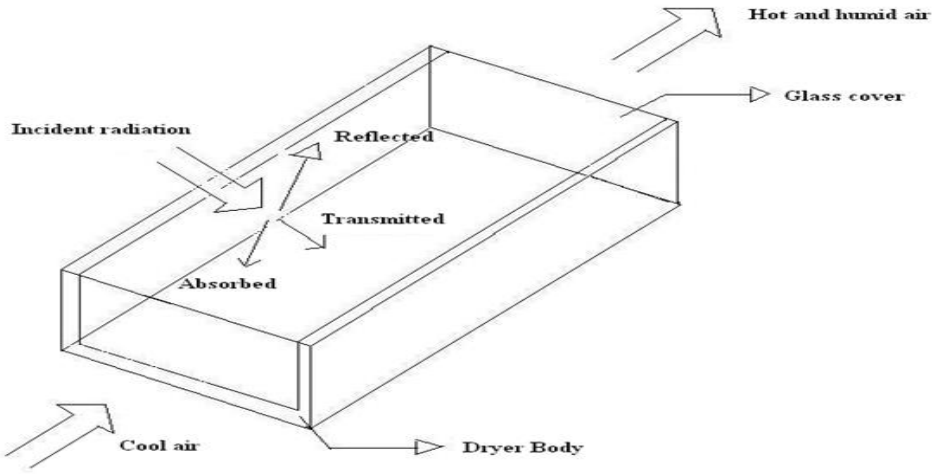

Figure 1. Diagram of a natural convection solar dryer

The dehydration methods are divided in four types: through contact with hot air; through contact with a hot surface; through liofilization; through the addition of osmotic agents. (Fioreze, 2003).

The considered solar dryer uses the first and second methods. The heat that provokes the dehydration of the fruits is transferred to them by the hot air that circulates inside the solar dryer and the inferior surface that becomes hot due to the radiation that passes through the glass cover of the equipment. So, the heat transfer processes involved in this analysis are: convection and radiation.

The solar radiation is electromagnetic, and the Earth receives this radiation in small wave lengths and emits in big ones. When the incident solar radiation hits the dryer glass cover, part is absorbed and causes a temperature elevation in the interior of the dryer, with consequent elevation of the thermal energy, resulting in a radiation with large wave lengths and small frequencies. This radiation is withheld in the dryer interior, causing the greenhouse effect, responsible for providing heat to the working fluid that is inside the dryer's interior. (Souza, 2004)

The Solar dryer is constituted by the drying chamber that is a box painted in black color, in which the product to be dried is placed. On the top of it there is a transparent glass cover, and through the way of the box there is the cool air inlet and the hot and humid air outlet.

The solar drying systems can be classified in many ways. Figure 2 shows a classification of solar dryers and drying ways.

ISSN 2176-5480

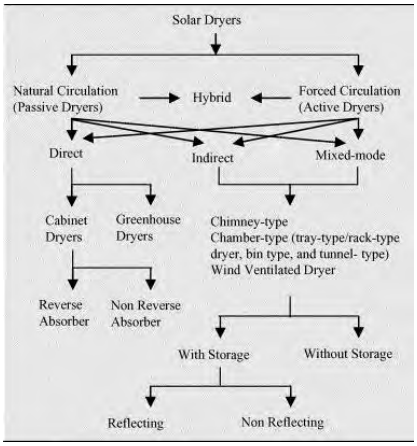

Figure 2. Classification of solar dryers and drying ways

It's possible to have a natural convection dryer with direct or indirect exposure and forced convection with direct or indirect exposure. What will determine its use are the resources available for the construction of the dryer. In the current case it's a natural convection dryer with direct exposure.

Natural convection refers to the case where convection of the fluid is driven only by local density variations, for example, in a closed box with a heat source. Natural and mixed convection flows and flows in which gravity is important can be modeled by the inclusion of buoyancy source terms. Buoyancy is driven by variations in density that can arise from a number of sources such as: local temperature variations that cause changes in the fluid density; variations in mass fractions in multiphase flows; variations in density in a general fluid; and local pressure variations for ideal gases and real fluids.

As the problem involves heat transfer between two parallel plates, buoyancy forces are more likely to drive the problem, formed by the difference of temperature between the hotter and cooler masses of air inside the dryer. Considering this, a study of this phenomenon influence in the considered case is necessary to understand the behavior of the studied equipment.

In vertical channels the buoyancy acts exclusively to induce the movement in the stream direction, then thermal boundary layers develop on each surface. If the canal is inclined there is a component of the buoyancy force in the normal direction of the current direction, as well as a component in the parallel direction.

According to Hewitt (1994), the relative importance of buoyancy forces due to temperature variations in convection flow can be estimated by using the ratio of Grashof and Reynolds Number:

$$\frac{Gr}{\mathrm{Re}^2} = \frac{g\beta L\Delta T}{U^2} \tag{1}$$

Where:

- β is the thermal expansion coefficient, 1/K.
- g is acceleration due to gravity m/s²
- L is the channel length, m
- ΔT is the difference of temperature between inlet and outlet, K
- U is the velocity in the considered direction, m/s

A value approaching or exceeding unity indicates that buoyancy effects are significant in the flow, while small values indicate that buoyancy effects can be ignored.

For many applications involving buoyancy, it is sufficient to assume a constant fluid density when the change in density over the expected range of conditions is relatively small. This is often true for many liquids. When the fluid density is not a function of pressure or temperature, the Boussinesq model is employed.

The Boussinesq model uses a constant density fluid model, but applies a local gravitational body force throughout the fluid that is a linear function of fluid thermal expansivity, β, and the local temperature difference with reference to a datum called the Buoyancy Reference Temperature. It is necessary to specify the reference temperature as an approximate average value of the expected domain temperature. The Boussinesq model is used by default for single-phase, single component simulations with heat transfer, using a constant density general fluid, which is air in this case.

ISSN 2176-5480

For buoyant flows where the density variation is driven only by small temperature variations, the Boussinesq model is used. In this model, a constant reference density ρ_{ref} is used for all terms other than the buoyancy source term (Hewitt, 1994). The buoyancy source term is approximated as:

$$\rho - \rho ref = -\rho ref \times \beta(T - Tref) \quad (2)$$

Where: T_{ref} is the buoyancy reference temperature (K), T is a local temperature (K) and β is given by:

$$\beta = -\frac{1}{\rho}\frac{\partial \rho}{\partial T} \mid P \quad (3)$$

The study to determine the most applicable turbulence model included a preliminary study over the transition in the thermal boundary layer associated to the process. The transition in the boundary layer in natural convection processes depends on the magnitude of the buoyancy and viscous forces developed on the fluid. According to Bejan (1984), in purely natural convection problems, the Rayleigh number indicates the relative strength of the buoyancy induced flow. The laminar flow regime is generally characterized by $Ra < 10^8$, while turbulent buoyant flow is characterized by $Ra > 10^{10}$. This dimensionless number is given by:

$$Ra, x = Gr, x \times \Pr = \frac{g\beta(Ts - T\infty)x^2}{\upsilon\alpha} \quad (4)$$

Where:

- x = Characteristic length (in this case is corrected due to the inclination of the plates), m
- Ra_x = Rayleigh number at position x
- T_s = Surface temperature (temperature of the wall), K
- T_∞ = Quiescent temperature (fluid temperature far from the surface of the object), K
- ν = Kinematic viscosity, m²/s
- α = Thermal diffusivity, m²/s
- Gr_x = Grashof number
- Pr = Prandtl number

Grashof and Prandtl numbers are dimensionless numbers that measure respectively the ratio between buoyancy and viscous forces and the ratio between moment and thermal diffusivity. They will be also useful in this case, to take some conclusions about the working regime of the solar dryer and about flow characterization.

The time dependence of the flow characteristics can be specified as either steady state or transient. Steady state simulations, by definition, are those whose characteristics do not change with time and whose steady conditions are assumed to have been reached after a relatively long time interval. They therefore require no real time information to describe them. Many practical flows can be assumed to be steady after initial unsteady flow development.

Transient simulations require real time information to determine the time intervals at which the flow field is calculated. Transient behavior can be caused by the initially changing boundary conditions of the flow, as in start up, or it can be inherently related to the flow characteristics, so that a steady state condition is never reached, even when all other aspects of the flow conditions are unchanging. Many flows, particularly those driven by buoyancy, do not have a steady state solution, and may exhibit cyclic behavior. If oscillatory behavior of the residual plots occurs while running a simulation in steady state option, this could be an indication of transient behavior.

In a transient analysis it's necessary to establish the total time that is the total duration, in real time, for the simulation, the time step that is the time increment until the total time is reached and the initial time for the simulation. The time step number is determined approximately by:

$$Timestep \cong 3 \times \frac{\Delta x}{v} \quad (5)$$

Where:

- Δx = mesh spacing in the flow direction, m
- v = previously encountered speed in the flow direction, m/s

ISSN 2176-5480

According to Souza (2004), the thermal efficiency of a solar dryer is given by:

$$\eta = \frac{\dot{m} Cp \Delta T}{IA} \tag{6}$$

Where:

- $\dot{m}$ = mass flow, kg/s
- C_p = specific heat, J/kg.K
- ΔT = temperature variation, from inlet to outlet, K
- I = incident solar energy, W/m^2
- A = glass cover area, m^2

According to Incropera et al. (2007), the Nusselt number, that is the ratio of convective to conductive heat transfer across (normal to) the boundary, for horizontal and inclined plates is given by the following correlation:

$$\overline{NuL} = 0.15 RaL^{1/3} \tag{7}$$

3. MATERIALS AND METHODS

The considered equipment consists of a body painted in black color, and a glass cover. Because of such simple geometry, it is possible to model the dryer as a channel formed by parallel plates, with two openings to the ambient. The thermal conditions on these surfaces can be idealized as isothermal or uniform thermal flux. The dimensions of the dryer are: 1500mm length, 490mm width and 60mm height. The built equipment is shown in Fig. 3.

Figure 3. Already built equipment drying apples and pears

To feed the computational model, the temperatures on the walls that correspond to the bottom of the solar dryer (which will receive the fruits), on the glass cover and on the laterals of the body were obtained in performed measurements on the real dryer using a K type (Chromel/alumel) thermocouple. Data for the bottom and glass cover were collected in nine points, near the lower opening, in the middle and near the upper opening. The obtained data is shown in Fig. 4, and it was obtained in a test performed at 11:00am with a solar radiation of 944.0 W/m².

ISSN 2176-5480

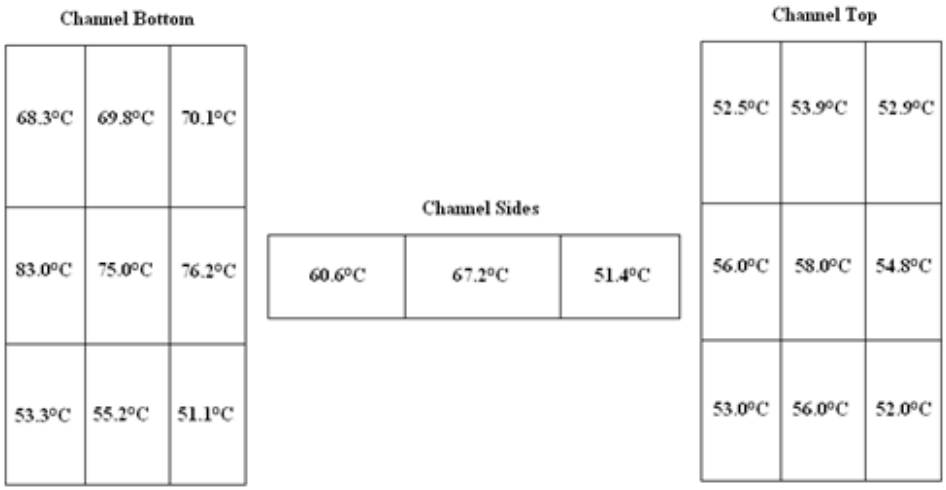

Figure 4. Temperatures obtained in performed test with the real dryer

Data corresponding to the air relative humidity in both openings were also measured, in order to check if there is air saturation on the exit of the hot and humid air. If so, optimization will include this factor as an important consideration. For the test day, at 11:00am, the air relative humidity on the dryer inlet was 66% and 81% on the outlet.

In the drying process is important to observe that the maximum insolation position, which means approximately perpendicular insolation during all the year, corresponds to 15,5° (Souza, 2004) for Natal city. Such inclination was adopted for the present computational model. Also, this study was performed considering a model of dryer that neglects the presence of the fruits on the channel, which means the attention was concentrated in heating exchange processes, not in the drying process itself.

The first step for obtaining the computational model for the studied dryer was using a 3D CAD Design Software (SolidWorks®) to draw the fluid domain that corresponds to the air inside the dryer.

The next step was to generate a computational mesh over the obtained geometry. It was imported to Ansys ICEM CFD® where the mesh was obtained creating blocks orienting it with the geometry and then associating the vertices and edges with the block. As it is a simple geometry, consisting of a simple channel composed of parallel plates, no problem was encountered in this step. The bottom, top and side parts of the channel were divided in three parts to make it possible to apply the different prescript temperatures in different regions, obtained in experimental tests, as boundary conditions. The resulting mesh is shown in Fig. 5.

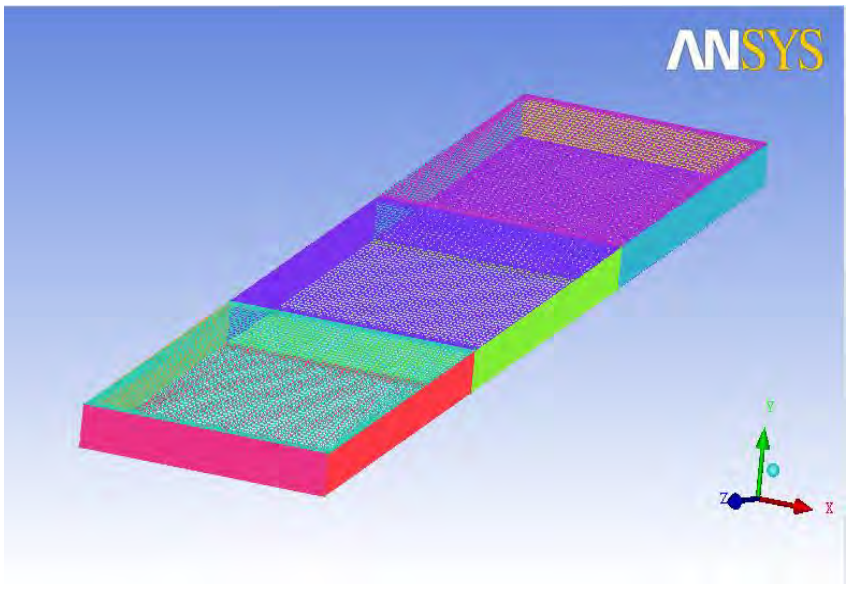

Figure 5. Obtained mesh from the previous geometry on Ansys ICEM CFD®

The following step is to import the generated mesh into Ansys CFX Pre® and prepare it to be used to solve the considered situation. The boundary conditions are established first.

ISSN 2176-5480

The lower and upper openings are opening boundary types, since it allows air to come in and out. If the regime was forced convection, then an inlet and outlet with known velocity would be adopted. The flow regime is subsonic, its direction is normal to the boundary condition, the relative pressure is 0 Pa and the opening temperature is 32°C, which is the one obtained from a solarimetric station installed in LMHES-UFRN.

The boundary conditions of the channel are of walls, with no slip model. The prescript temperatures used were an average of the three measured for each section (for bottom and glass cover), previously obtained in tests and shown in Fig. 4.

After this stage, the default domain is specified. The material is air at 25°C and the fluid is assumed to be continuous. The buoyancy is turned on, being specified the direction and magnitude of the gravity vector and the buoyancy reference temperature (32°C), already explained in the bibliographic revision.

To check if there is turbulence present in this problem, the Rayleigh number is calculated as indicated by Eq. 4.

$$Ra, x = \frac{g\beta(Ts - T\infty)x^2}{\upsilon\alpha} = \frac{9.81 \times \frac{2}{(351+305)} \times (351-305) \times 1{,}5^3}{20.92 \times 29.9 \times 10^{-12}} = 7.423 \times 10^9$$

The heat transfer model used was Thermal Energy and the turbulence was neglected, because the calculus of the Rayleigh number showed that the process occurs without thermal transition in the boundary layer to a turbulent flow regime ($Ra < 10^{10}$). The initialization was made zeroing the values corresponding to the velocity Cartesian components, the relative pressure and the temperature.

The analysis type in the first run was considered steady state. The first values obtained showed a characteristic oscillatory behavior of the residual plots, being an indication of a transient behavior. The analysis type was, then, changed to transient. For the transient analysis, the total time was considered 55 seconds and the time step calculated was approximately 0.05 seconds. After assuming this, the case is ready to be solved, defining the simulation to be run in the Ansys CFX Solver®. The final case in Ansys CFX Pre® can be visualized in Fig. 6.

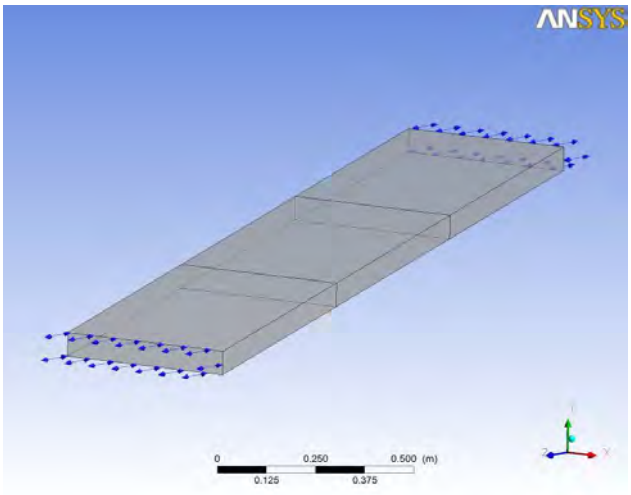

Figure 6. Case configured in Ansys CFX Pre® ready to be simulated

4. RESULT ANALYSIS

After the run, the software returns a lot of variables related to the boundaries of the default domain such as viscous and pressure moment and forces on walls. What are sought in the present article are variables related to the fluid itself as: U-Mom, V-Mom, W-Mom, P-Mass, H-Energy, and much other as dynamic viscosity, velocity, Rayleigh number, thermal conductivity, thermal expansivity and specific heat capacity at constant pressure. With such data is possible to study the properties of the dryer.

ISSN 2176-5480


```
================================================================================
              Boundary Flow and Total Source Term Summary
================================================================================

+------------------------------------------------------------------------------+
|                        Average Scale Information                             |
+------------------------------------------------------------------------------+

Domain Name : Default Domain
    Global Length                                  = 3.5840E-01
    Minimum Extent                                 = 4.6586E-01
    Maximum Extent                                 = 1.4454E+00
    Density                                        = 1.1850E+00
    Dynamic Viscosity                              = 1.8310E-05
    Velocity                                       = 2.5628E-01
    Advection Time                                 = 1.3985E+00
    RMS Courant Number                             = 3.6188E+01
    Maximum Courant Number                         = 3.8945E+02
    Reynolds Number                                = 5.9444E+03
    Thermal Conductivity                           = 2.6100E-02
    Specific Heat Capacity at Constant Pressure    = 1.0044E+03
    Thermal Expansivity                            = 3.3560E-03
    Prandtl Number                                 = 7.0462E-01
    Temperature Range                              = 4.6011E+01
    Rayleigh Number                                = 2.0581E+08
    Buoyancy Time                                  = 6.3507E-01
```

Figure 7. The more relevant data returned by the software.

First, observing the returned average Rayleigh number that corresponds to 2.0581e+08 it is proven that no turbulence occurs, as it was considered previously. Nusselt number is, then, calculated through Eq. 7 as shown below:

$$\overline{NuL} = 0.15RaL^{1/3} = 0.15 \times (2.0581)^{1/3} = 88.56$$

With these data, it is also possible to calculate Grashof number that, as shown in Eq. 4, consists of the division of Rayleigh number for Prandtl number. The result found is 2.9209e+08.

Using Ansys CFX Post® it is possible to visualize, by the use of planes and streamlines, properties as pressure, temperature, vorticity, velocity and its independent components, etc. What was done was create YZ planes and color them with contours of specified temperatures. Those temperatures were 32°C (ambient temperature, minimum fluid domain temperature) and 78°C (maximum temperature of the fluid domain). With so, it was possible to visualize what was the actual temperature on each section of the fluid domain at each time step and observe its change with the advance of the total time. Figure 8 and fig. 9 shows the resulting post of the results at 55 seconds. Figure 9 has an additional streamline to show the movement of the air particles inside the fluid domain and their temperature along the way out of the dryer, showing the thermal boundary layers on the channel walls.

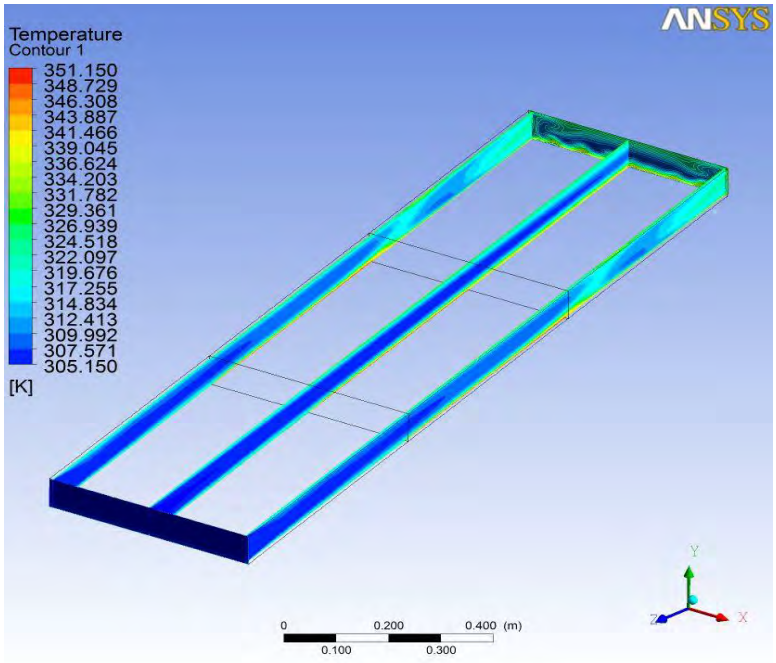

Figure 8. Temperature gradient developed on the air inside the solar dryer when steady state is reached

ISSN 2176-5480

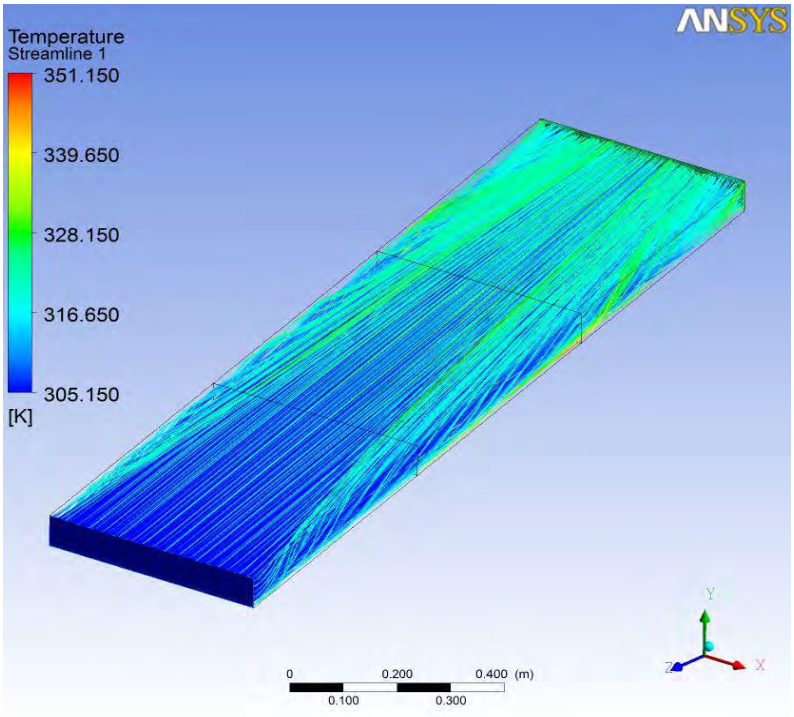

Figure 9. Movement and temperature of the air particles that are inside the solar dryer when steady state is reached.

In Fig. 10 is possible to observe the development of the thermal boundary layers associated to the contact of the working fluid (air) with the channel hot walls. It is also possible to see that the temperature profile is becoming fully developed, reaching higher temperature averages on the latest sections of the dryer, what consists of an advantage for the drying process.

With the function calculator feature of CFX Post, it is possible to calculate the difference of the product of mass flow and temperature considering the two openings. The mass flow integral of temperature on the lower opening corresponds to 2.88692 K.kg/s. The same variable on the upper opening has the value of 3.00878 K.kg /s. It was also possible to obtain the area that is responsible for receiving the solar radiation, or the glass cover area. It corresponds to 0.735m². As already said on the bibliographic revision, the solar dryer efficiency is given by:

$$\eta = \frac{\dot{m} Cp \Delta T}{IA} = \frac{Cp \times [(\dot{m}T)out - (\dot{m}T)in]}{IA} = \frac{1.044 \times (3.00878 - 2.88692)}{944 \times 0.735} = 18.33\%$$

The velocity vectors and pressure gradients were also analyzed. As shown in fig. 10 and fig. 11, the velocities and pressure suggest that the hot air comes out through the upper opening and cooler one goes in through the lower one. This means that the hotter mass of air that is found in the latest sections of the solar dryer, tending to have a lower density, is dragged out generating a local lowering of pressure, responsible for drawing ambient air into the drying chamber.

ISSN 2176-5480

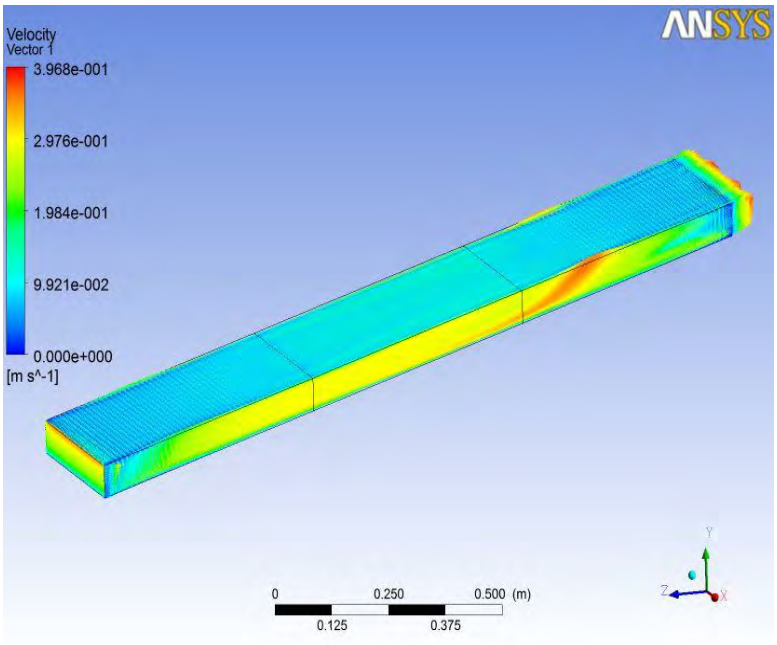

Figure 10. Local velocity vectors associated to the flow

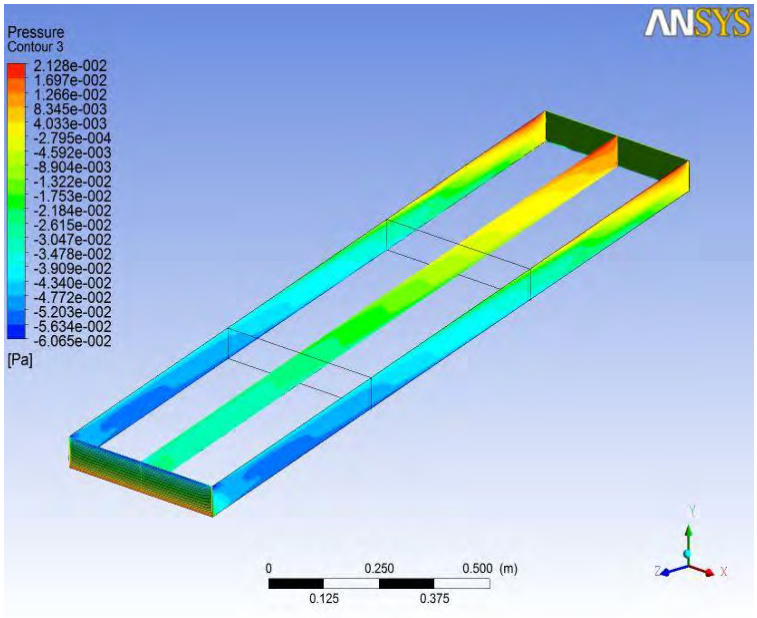

Figure 11. Local pressure gradient

The relative importance of buoyancy forces due to temperature variations in convection flow can be estimated by using Eq. 1:

$$\frac{Gr}{\mathrm{Re}^2} = \frac{2.9209 \times 10^8}{(5.9444 \times 10^3)^2} = 8.27$$

As the ratio is approximately 8.27 times unity, the buoyancy forces due to temperature variations exert significant influence over the developed flow.

ISSN 2176-5480

5. CONCLUSIONS

1. The studied solar dryer does not present thermal boundary layer transitions, proven after obtained Rayleigh number and after visualization of the streamline;
2. For the studied case it was proven that the buoyancy drives the problem, proven through previous analysis of the velocity vectors and pressure gradients, through the Grashof number, which indicates that the buoyancy forces are much more significant than the viscous forces in this case and through the ratio between Grashof and Reynolds number, that indicated a significant influence of buoyancy forces in the convection flow;
3. For this case, the thermal diffusivity is more significant than the moment diffusivity, as shown by the Prandtl number, that is less than unity.
4. For the considered process, as shown by the Nusselt number, the convective heat transfer is dominant over the conductive.
5. The studied solar dryer showed itself feasible for the obtaining of dried fruits, having an efficiency above of what is shown on literature;
6. As the air did not saturate in the drying processes and the flow temperatures profile is tending to become fully developed in the upper part of the drying chamber, it is possible to see that if the dryer had a greater length, the temperatures reached would be higher and the drying process would be optimized;
7. The initial section of the dryer is submitted to lower temperatures but, as the air is less saturated at inlet, the difference of mass transfer between the different sections is negligible;
8. Other simulations together with experimental test are necessary to determine a geometry that promotes reasonable efficiency in transmitting the incident energy to the working fluid and also reasonable drying efficiency.

6. REFERENCES

A. Bejan, 1984, Convection Heat Transfer, John Wiley & Sons, New York.
Incropera, F.P., DeWitt, D.P., Bergman, T.L., Lavine, A.S., 2007, Fundamentals of Heat and Mass Transfer, Sixth Edition, John Wiley.
Hewitt G. F, Shires, G. L., Bott T. R., 1994, Process Heat Transfer, CRC Press, Boca Raton,.FL, USA.
Duffie, J.A., Beckman, W.A., 1991, Solar Engineering of Thermal Processes, Second Edition, New York, John&Sons, & Beckman.
Machado, A. V., 2009, Estudo da Secagem do Pedúnculo do Caju em Sistemas Convencional e Solar: Modelagem e Simulação do Processo, Dissertação de Mestrado do Programa de Pós-Graduação em Engenharia Química da UFRN, Natal.
Fioreze, R., 2003, Princípios da Secagem de Produtos Biológicos. João Pessoa, Editora da Universidade Federal da Paraíba – UFPB.
Meloni, P.L.S., 2002, Manual de Produção de Frutas Desidratadas, Instituto de Desenvolvimento da Fruticultura e Agroindústria – Frutal/ Sindicato dos Produtores de frutas do Estado do Ceará – Sindifruta.
Souza, L.G. M, 2004, Secador Solar a Baixo Custo para Frutas Tropicais, CONEM-2004, Belém/PA.
Neto, H. J. L., 2008, Obtenção de Tomate Seco Através do Uso de um Sistema Solar Alternativo de Baixo Custo, Dissertação de Mestrado do Programa de Pós-Graduação em Engenharia Mecânica da UFRN, Natal.
EMBRAPA - Empresa Brasileira de Pesquisa Agropecuária, Tomate para processamento industrial, Brasília, DF, 2000.

7. RESPONSIBILITY NOTICE

The authors are the only responsible for the printed material included in this paper.